Fermilab

Doc Number: Beams-doc-4896
Version: 2.00
Category: Note

Collimation Design using Reduced Courant-Snyder Coordinates

Bruce C. Brown
Accelerator Division, Main Injector Department
Fermi National Accelerator Laboratory *
P.O. Box 500
Batavia, Illinois 60510

27 May 2016

Contents

*Operated by the Universities Research Association under contract with the U. S. Department of Energy

Abstract

An effective explanation for the design of a primary-secondary collimator system may employ a diagram in reduced coordinates. We construct such a diagram for the Main Injector collimation system and illustrate how much of the beam which is scattered by the primary collimator is absorbed in the first turn by the nearby secondary collimators. Additional losses are captured in subsequent turns following which some of the initially scattered beam will strike the primary collimator and be rescattered.This note will document the parameters for this system to confirm the various magnitudes and their relationships. We find for an 8-GeV beam that a 3-σ horizontal beam size of 9.35 mm is scattered by a 0.25 mm Tungsten blade to give an RMS scattering angle of 371 μradians giving a size $\sqrt{\beta * 50)}\Theta_0 = 15.95$ mm which makes the great effectiveness of the Main Injector collimation system seem quite reasonable.

1 Introduction

Linear motion in a strong focusing lattice can be transformed to coordinates in which the motion is described as a circle. For horizontal motion one has $(x, \beta_x x' + \alpha x)$ or $(x/\sqrt{\beta_x}, (\beta_x x' + \alpha x)/\sqrt{\beta_x})$. To provide consistent units of mm we further normalize the β_x by a typical β of 50 m resulting in the form $(x/\sqrt{\beta_x/50}, \sqrt{50\beta_x}x' + \alpha x/\sqrt{\beta_x/50})$. We begin with particles at the 3-σ boundary of the beam and scatter them with a 0.25 mm Tungsten (W) foil. We then plot the coordinates for the 1-σ (in scattering angle) scattered beam at the scattering point and at the phase advance corresponding to secondary collimators S1 (C301), S2 (C303), S3 (C307), and S4 (C308).

2 Scattering

We employ the standard small angle multiple scattering formalism described by the Particle Data Group. $\Theta_0 = \Theta_{plane}^{RMS}$ provides the desired scattering amplitude.

$$\Theta_0 = \frac{13.6MeV}{\beta cp} z \sqrt{\frac{x}{X_0}} [1 + 0.038 \ln \frac{x}{X_0}] \tag{1}$$

where

- β is $v/c = 0.9945$, $p = 8.8886$ GeV/c is the momentum
- $\beta cp = 8.8396$ GeV for the 8 GeV Booster Beam

- $z = 1$ (particle charge)
- $x = 0.25$ mm
- $X_0 = 6.76$ g/cm^2 or $X_0 = 3.5$ mm
- $\frac{x}{X_0} = 0.0714$
- The term in the bracket calculates as 0.8997
- $\Theta_0 = 3.7 \times 10^{-4}$ radians

For the Main Injector primary collimator, CPH230, we use Courant-Snyder lattice parameters of $\beta_{CS} = 37$ m, $\alpha_{CS} = 2.55$, we find the amplitude for the beam which experiences a 1-σ scattering angle to be

$$\sqrt{50\beta_{CS}}\Theta_0 = 15.95\ mm \tag{2}$$

3 Emittance

We normally employ the emittance (ϵ_{95}) which contains 95% of the particles. We calculate the RMS beam size and then express a beam boundary at a ratio to the RMS size.

$$\sigma_x = \sqrt{\frac{\beta_{CS}\epsilon_{95}}{6\beta\gamma}} \tag{3}$$

where the 6 is due to using 95% emittances, $\beta\gamma$ is the relativistic factor for the beam. Assuming $\epsilon_{95} = 15$ pi-mm-mr, we find $\sigma_x = 3.12$ mm or $3\sigma_x = 9.35$ mm.

A proton scattered from the $3\sigma_x$ edge of the circulating beam by the angle $\pm\Theta_0$ will thereafter travel along the circle of emittance $6.19\sigma_x$ relative to the initial beam. Protons with smaller scatting will fill the region between these circles while the remaining beam with larger scattering angle will be outside (thereby more easily collimated).

4 Phase Plots

Figure 1 illustrates the scattering and the position of scattered particles in the normalized phase plot at each of the secondary collimators. We plot the scattering point on the positive x axis and show the beam scattered by 1-σ as vertical lines (green for beam scattered to positive angles (out scatter)and

red beam scattered to negative angles (in scatter)). We follow this beam to the horizontal phase advance (clockwise is positive) corresponding to the four secondary collimators: 156.3, 244.21, 427.71, and 474.47 degrees. In this description, the phase advances in a clock-wise fashion. Here we employ a right-hand coordinate system in z along the beam direction, y up and therefore positive x is to the inside of the Main Injector.

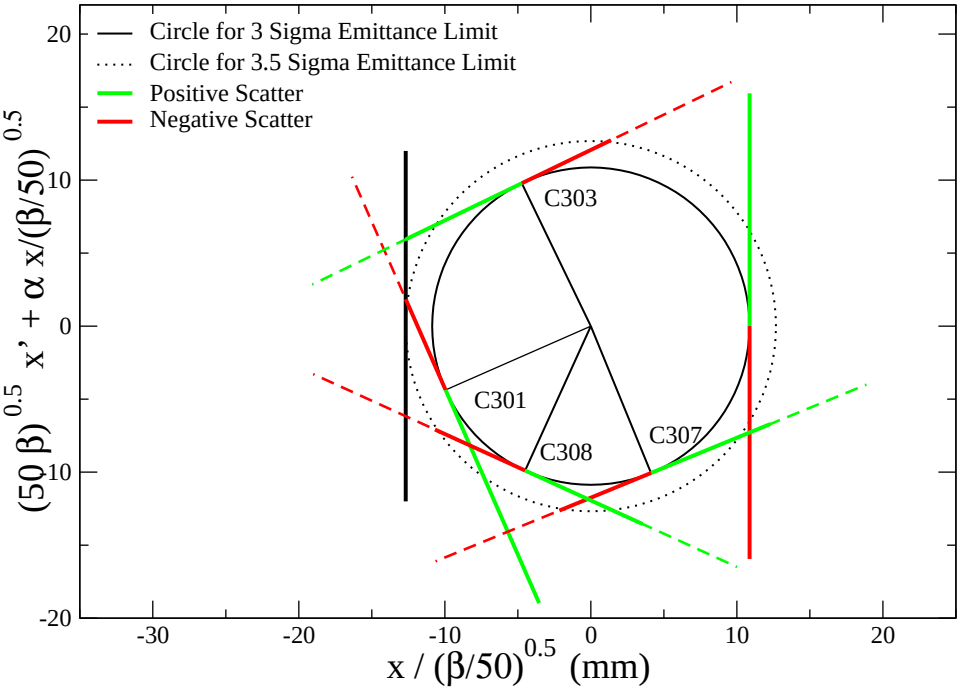

Figure 1: Normalized coordinate plot of beam which is scattered at the primary collimator as it appears at the four secondary collimators. The vertical axis is offset to neglect the αx term. This figure is a circle, despite whatever success or lack thereof we have in properly scaling the computer plots. The portion of the negative scattered beam which is collimated at C301 is shown with dashed red while the positively scatter beam collimated at C303 is shown with the dashed green line.

The primary collimator is placed to intercept particles which fail to be accelerated so they fall to the inside. We place the horizontal edge of the primary at positive $3\sigma_x$ boundary. We tuned-up the Main Injector collimation system for operation in 2008-2012 to place the horizontal edge for C301, C303, and C307 on the radial outside (negative) with the C308 edge

on the inside (positive). Each secondary collimator was moved toward the beam until it limited transmission resulting in placing them near the $3.5\sigma_x$ boundary. We show the solid green and red lines of scattered particles at the primary. Portions intercepted by C301 or C303 are then shown by replacing the solid lines by dashed lines. On the first turn, C307 and C308 do not intercept additional scattered particles.

The collimation system provided the limiting aperture in the Main Injector. Apertures in the rest of the Main Injector permitted the scattered particles to circulate many turns. The STRUCT simulations indicated that the collimated particles struck the primary on average 2.6 times on their way to capture with 99% efficiency. We illustrate the subsequent turns for a horizontal tune of 26.415 in Figure 2. [The nominal design for the Main Injector uses a horizontal tune of 26.425] For illustration we show the particles which struck the primary but scattered at a zero angle with a circle.

With a primary collimator at the positive $3\sigma_x$ boundary, we strike on turn 0 as shown. At turn 5 we are nearly at that boundary and many particles which were initially scattered inward (negative) and not captured will strike the scattering foil (primary collimator) again. On turn 7 we observe that the positive scattered particles may again be scattered. Note that the secondary collimators are at the $3.5\sigma_x$ boundary leaving particles for the primary which is at the $3\sigma_x$ boundary. [We designate turn 1 to start just after scattering on the primary at turn 0].

For C301, we see (as shown in Figure 1) that it is placed to intercept beam on turn 1 (negative scatters) and again on turn 3 (positive scatters). It will also be very effective on turn 8 for the rescattered particles.

For C303, we find significant capture on turn 1 for positive scattered particles. Perhaps additional of these may be caught on turn 6 and for rescatters on turn 11. It will also be effective for negative scatters on turn 4.

For C307 we see, as we knew already, that this secondary is less effective for the uncaptured beam we scatter at the primary. It might have some effect for negative scatters on turn 3 and is well positioned to capture on turn 5 and turn 10.

For C308 (near beam on positive edge) we expect loss capture on turn 2 and again on turn 4 and turn 9.

Please note that the STRUT simulations accounted for all of these effects plus others in guiding us to this design.

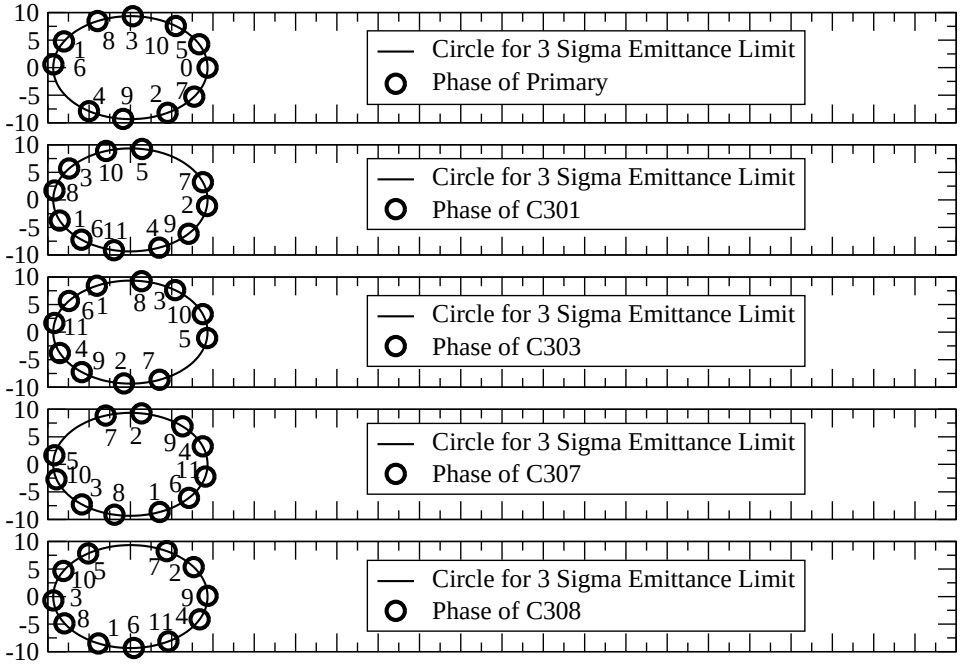

Figure 2: Normalized coordinate plot of beam which is scattered at the primary collimator as it appears at the four secondary collimators. The vertical axis is offset to neglect the αx term. This figure is a circle, despite whatever success or lack thereof we have in properly scaling the computer plots. The particles striking the primary collimator but not scattering are followed for the next eleven turns. Each collimators is considered separately.

5 Final Comments on the Collimator Locations

If this is your introduction to the MI Collimators, our choices for collimator placement might seem strange. Actually, we were very constrained and the fortunate success of these collimators is despite fundamental limitations. Only limited space is available due to filling almost all the tunnel with dipoles and quadrupoles. The uncaptured beam was distinguished by following a dispersion orbit to the inside of the beam at locations where the dispersion is sufficiently large. CPH230 is upstream of the MI300 straight section where there was space for secondary collimators. It has nearly the nominal dispersion. C301 is in the first 'open' space downstream of CPH230. C303 is not quite the next available space. Then we needed to provide enough absorber in masks to protect sensitive equipment used for ECOOL in the

Recycler. C307 is just downstream of the ECOOL region. C308 is then near the end of the available free space the MI300 since dipoles resume downstream of Q309.

6 Acknowledgments

As we prepare to design a collimation system for the Recycler, we are more than ever in appreciation for the above design provided by Alexandr Drozhdin. Assistance with normalized coordinates was obtained from John Johnstone and Phil Adamson.